SLAC – PUB – 3622
April 1985
(T/E)

POLARIZED $-e^{\pm}$ p SCATTERING IN A SUPERSYMMETRIC ELECTROWEAK MODEL*

LUC MARLEAU†

Stanford Linear Accelerator Center
Stanford University, Stanford, California, 94305

ABSTRACT

The polarization and charge asymmetries in the scattering of longitudinally polarized electron by proton are considered in the context of a supersymmetric extension of the standard model. The contribution of the subprocess $eq \to \tilde{e}\tilde{q}$ followed by the fast decay of $\tilde{e} \to e\tilde{\gamma}$ is computed for various sets of superpartner masses at energies corresponding to the ep collider at HERA (30 GeV $\times$ 820 GeV) and to an hypothetical ep machine at SSC (30 GeV $\times$ 20 TeV).

Submitted to *Physical Review D*

* Work supported by the Department of Energy, contract DE – AC03 – 76SF00515.
† Address after June 1, 1985: Département de physique, Université Laval, Québec, P.Q., Canada, G1K 7P4.

1. Introduction

Despite the striking success of the standard $SU(3) \times SU(2) \times U(1)$ gauge model of the strong, weak and electromagnetic interactions, many questions remain unanswered: the problems of fermion generations is not addressed; one would like to include gravitational forces; and, in general, there are too many parameters in the theory (in the form of coupling constants and fermion masses and mixings). An obvious way to reduce the number of parameters is by introducing more symmetry to the theory. Such is the case in supersymmetric extensions of the standard model.

Supersymmetry[1,2] (SUSY) is a natural extension of gauge theories which is less divergent and mathematically better behaved. One of the major properties of SUSY is to associate to each particle, a partner which spin differs by 1/2. Up to now no supersymmetric particle has been found, the present experimental status permitting only to set lower bounds on some of their masses. When one reaches higher energies, and superpartners are produced, clearly the whole spin content of the theory is changed. Keeping this fact in mind, it would be most instructive to examine polarized processes in SUSY extensions of the standard model.

Perhaps the best place to look up for such effect is in neutral current processes, for example in deep inelastic

$$e^-_{L,R}\, p \to e^- X \tag{1.1}$$

In the past, this process has proven to provide a good test of the standard model and a way to determine the Weinberg angle, θ_W.[3]

In this work we examine how polarization effects are expected to differ from the standard model predictions when one consider the contribution of the subprocess

$$e^-_{L,R} + q \to \tilde{e}^- + \tilde{q} \qquad (1.2)$$

to (1.1) where $\tilde{e}$ and $\tilde{q}$ are the selectron and squark respectively. Unlike previous studies[4,5] of process (1.2) the selectron is assumed to decay very fast into

$$\tilde{e}^- \to e^- \tilde{\gamma} \qquad (1.3)$$

with a very light photino, $\tilde{\gamma}$, going undetected. The result is a process which, experimentally, looks much like electron-quark scattering except for the missing momenta carried by the photinos. Based on experimental evidence and depending on the SUSY breaking mechanism, the $\tilde{e}$ and $\tilde{q}$ masses are believed to be in the range 20 GeV $\lesssim m_{\tilde{e}},\ m_{\tilde{q}} \lesssim$ 100 GeV. The electron ring at HERA will have the ability to produce longitudinally polarized electrons with sufficient energy to span at least part of this range when it starts running in 1990.

The paper is organized as follows: We review the basic elements of deep inelastic *ep* scattering and define various polarization and charge asymmetries in Section 2. In Section 3, we address the question of gauge fermion mass mixings and then examine the contribution of (1.2) – (1.3) to the $e^{\pm}_{L,R}\ p \to e^{\pm} X$. Numerical results are presented for various sets of superpartners masses in Section 4. We examined two experimental scenarios, the first one is HERA, the second one, an hypothetical *ep* collider at the Superconducting Super Collider (SSC). Section 4 also contains some general conclusions.

2. Polarization in Deep Inelastic *ep* Scattering

We begin by defining the usual kinematical variables associated with deep inelastic scattering:

$$x = Q^2/2M_p s \ ,$$
$$y = Q^2/xs \ ,$$

with

$$\begin{aligned} s &= (p + p_1)^2 \ , \\ Q^2 &= -t = -(p_3 - p_1)^2 \ , \\ \nu &= p \cdot q/s \ , \end{aligned} \tag{2.1}$$

where p, p_1, p_3 are the momenta of the proton, and the incoming and scattered electron respectively, $q \equiv p_3 - p_1$ and M_p in the mass of the proton.

In the quark parton model, polarized $-ep$ scattering ($e^-_{L,R}\ p \to eX$) is interpreted as electron-quark collisions:

$$e^-_{L,R} + q_i(\bar{q}_i) \to e^- + q_i(\bar{q}_i) \ . \tag{2.2}$$

When the quark and the electron are both left– or right–handed, one finds the differential cross section

$$\frac{d\hat{\sigma}_{AA}}{d\hat{t}} = \pi\alpha^2 \left| \frac{a}{\hat{t}} + \frac{b_{AA}}{\hat{t} - M_Z^2} \right|^2 \ , \tag{2.3}$$

where a and b_{AB} are defined as:

$$\begin{aligned} a &= Q_e Q_i \\ b_{AB} &= Q^Z_{Ae} Q^Z_{Bi} \qquad \text{with } A, B = L, R \ . \end{aligned} \tag{2.4}$$

$\overline{Q}_f$ denotes the electric charge of the fermion f and, Q^Z_{Rf} and Q^Z_{Lf} the right– and left–handed Z^0 charges respectively. Variables denoted by a hat are as usual

associated with an elementary subprocess (e.g. $\hat{s} = -xs$). When the quark and the electron have opposite handedness

$$\frac{d\hat{\sigma}_{AB}}{d\hat{t}} = \pi\alpha^2 \left| \frac{a}{\hat{t}} + \frac{b_{AB}}{\hat{t} - M_Z^2} \right|^2 \cdot (1-y)^2 \ , \quad A \neq B \ . \tag{2.5}$$

The $e^- p$ cross section is then

$$d\sigma_A^{(-)} \equiv \frac{d\sigma_A^{(-)}}{dxdy} = s \sum_i x \ f_i(x, Q^2) \ \frac{d\hat{\sigma}_{iA}}{d\hat{t}} \ . \tag{2.6}$$

The summation runs over the quark flavors i, $f_i(x, Q^2)$ are the parton distribution functions in the proton and $d\hat{\sigma}_{iA}/d\hat{t}$ is the cross section for the subprocess (2.2) and therefore involves the average over left– and right–handed quarks.

The weak properties of the standard model are known to be directly exhibited in the polarization asymmetries $A^{\pm}$:

$$A^{\pm}(x,y) = \frac{d\sigma_R^{(\pm)} - d\sigma_L^{(\pm)}}{d\sigma_R^{(\pm)} + d\sigma_L^{(\pm)}} \ , \tag{2.7}$$

where we have generalized (2.6) to the case of the positron, with the obvious notation.

Following Ref. 6, we also define other useful tools to test the theory: The polarization asymmetries $B^{L,R}$

$$B^A(x,y) = \frac{d\sigma_A^{(-)} - d\sigma_A^{(+)}}{d\sigma_A^{(-)} + d\sigma_A^{(+)}} \ , \quad A = R, \ L \ , \tag{2.8}$$

and the charge asymmetry for unpolarized $e^{\pm} p \to e^{\pm} X$ scattering

$$C(x,y) = \frac{d\sigma^{(-)} - d\sigma^{(+)}}{d\sigma^{(-)} + d\sigma^{(+)}} \ . \tag{2.9}$$

3. Supersymmetric Effects

Let us first briefly review some of the characteristics of supersymmetric extensions of the standard model. They can be summarized as follows: A new spectrum of particles is introduced, the superpartners (e.g. selectrons ($\tilde{e}$), squarks ($\tilde{q}$), photino ($\tilde{\gamma}$), zino ($\tilde{Z}$) , higgsino ($\tilde{H}$), etc...). Their couplings with other particles are fixed . SUSY also predicts that the mass of the new particles should be equal to the that of the corresponding standard partners. But, since superpartners are yet to be found, one must assume that SUSY breaks down in the low energy limit. In general, this introduces more parameters in the theory such as the mass mixing between gauge fermions and the fermionic superpartners of the Higgs bosons, the higgsinos. In a minimal SUSY extension of the standard model, there are at least four neutral state mixing: $\lambda_{\tilde{\gamma}}$, $\lambda_{\tilde{Z}}$, $\psi^1_{H_1}$ and $\psi^2_{H_2}$ which are respectively the photino, zino and the two higgsino states. This means in our case (two Higgs) that in $eq \to \tilde{e}\tilde{q}$, the interactions can be mediated by the four mass eigenstates.

One can write the most general mass term as follows:[7]

$$\begin{aligned}\mathcal{L}_{M.T.} = & \frac{i}{2}(g^2+g'^2)^{1/2}\lambda_{\tilde{Z}}(v_1\psi^1_{\tilde{H}_1} - v_2\psi^2_{\tilde{H}_2}) \\ & + \frac{1}{2}(M\cos^2\theta_W + M'\sin^2\theta_W)\lambda_{\tilde{Z}}\lambda_{\tilde{Z}} + (M-M')\sin\theta_W\cos\theta_W\ \lambda_{\tilde{Z}}\lambda_{\tilde{\gamma}} \\ & + \frac{1}{2}(M'\cos^2\theta_W + M\sin^2\theta_W)\lambda_{\tilde{\gamma}}\lambda_{\tilde{Z}} + \mu\psi^1_{\tilde{H}_1}\psi^2_{\tilde{H}_2} + h.c.\end{aligned} \tag{3.1}$$

where g and g' are defined as usual

$$g'\cos\theta_W = g\sin\theta_W = e\ . \tag{3.2}$$

Furthermore, v_1 and v_2 are the vacuum expectation values of Higgs bosons H_1 and H_2 respectively, and M, M' and μ are mass parameters.

Let us consider, for simplicity, the case where $\mu = 0$ and $M = M'$ in (3.1). Working in the convenient basis

$$\psi_j^0 = \left(-i\lambda_{\tilde{\gamma}},\ -i\lambda_{\tilde{Z}},\ \frac{v_1\psi_{H_1}^1 - v_2\psi_{H_2}^2}{(v_1^2+v_2^2)^{1/2}},\ \frac{v_1\psi_{\tilde{H}_1}^1 + v_2\psi_{\tilde{H}_2}^2}{(v_1^2+v_2^2)^{1/2}} \right), \tag{3.3}$$

the mass terms of (3.1) can be rewritten

$$-\frac{1}{2}(\psi^0)^T\ Y\psi^0 + h.c. \tag{3.4}$$

with

$$Y = \begin{pmatrix} M & 0 & 0 & 0 \\ 0 & M & -M_Z & 0 \\ 0 & -M_Z & 0 & 0 \\ 0 & 0 & 0 & 0 \end{pmatrix} \tag{3.5}$$

The mass eigenstates are then easy to find by analyzing the non-trivial 2×2 submatrix of Y. One finds the mass eigenstates X_j^0:

$$X_j^0 = (\psi_1^0,\ \psi_2^0\cos\phi + \psi_3^0\sin\phi,\ i(-\psi_2^0\sin\phi + \psi_3^0\cos\phi),\ \psi_4^0), \tag{3.6}$$

with mass eigenvalues M, $\frac{1}{2}(m_0 + M)$, $\frac{1}{2}(m_0 - M)$ and 0 respectively where

$$\begin{aligned} m_0 &= (4M_Z^2 + M^2)^{1/2}\ , \\ \cos 2\phi &= \frac{m_0}{M}\ . \end{aligned} \tag{3.7}$$

In the limit $M \simeq 0$, the masses of the gauge fermions are equal to that of their standard partners. Experimentally, the $M \simeq 0$ limit (very light photino)

could be tested at HERA and we will base our discussion on that fact. The higgsino mixings in X_2^0 essentially disappear for that limit and the zino becomes an eigenstate of mass M_Z. That as may be, we shall not restrict our analysis to the sole case of $M_{\tilde{Z}} = M_Z$. The contribution from diagrams involving higgsinos as mediating the interactions will be ignored here; in $eq \to \tilde{e}\tilde{q}$ scattering, the higgsino couplings with the fermion and its superpartner can be neglected with respect to the gauge coupling for all practical purposes.

Consider now the subprocess

$$e_{L,R}(p_1) + q_i(p_2) \to \tilde{e}(p_3) + \tilde{q}_i(p_4), \tag{3.8}$$

where the SUSY electroweak interactions are mediated by the photino $\tilde{\gamma}$, and the zino, $\tilde{Z}$ (see Fig. 1(b)). The interaction vertices are described by the Feynman rules of Fig. 2.[7] Summing over the final states helicities one finds the matrix elements:

$$|T^{AA}|^2 = 4e^4\hat{s}\left[\frac{M_{\tilde{\gamma}}a}{\hat{t}_{13} - M_{\tilde{\gamma}}^2} + \frac{M_{\tilde{Z}}b_{AA}}{\hat{t}_{13} - M_{\tilde{Z}}^2}\right]^2 , \tag{3.9}$$

for initial particles having the same handedness and for $A \neq B$,

$$|T^{AB}|^2 = 4e^4 \cdot [-(m_3^2 - \hat{t}_{13})(m_4^2 - \hat{t}_{13}) - \hat{s}\hat{t}_{13}] \cdot \left[\frac{a}{\hat{t}_{13} - M_{\tilde{\gamma}}^2} + \frac{b_{AB}}{\hat{t}_{13} - M_{\tilde{Z}}^2}\right]^2 , \tag{3.10}$$

where m_3 and m_4 are the selectron and squark masses respectively and $\hat{t}_{13} = (p_1 - p_3)^2$. As before, we neglected the electron and quark masses with respect to m_3 and m_4 (20 GeV $\lesssim m_3,\ m_4 \lesssim$ 100 GeV).

In (3.9-10), $\tilde{\gamma}$ and $\tilde{Z}$ are assumed to be the mass eigenstates discussed earlier. In general when $M \neq M'$ in (3.1), $\tilde{\gamma}$ and $\tilde{Z}$ are no longer decoupled but (3.9)

and (3.10) can be generalized easily for gauge fermion mass eigenstates α and β as follows:

$$a \to a = Q^{\alpha}_{Ae}\, Q^{\beta}_{Bi}\ ,$$

$$b_{AB} \to b_{AB} = Q^{\alpha}_{Ae}\, Q^{\beta}_{Bi}\ , \tag{3.11}$$

$$M_{\tilde{\gamma}},\ M_{\tilde{Z}} \to M_{\alpha}\, M_{\beta}\ .$$

Under the assumption that the photino is the lightest and most stable SUSY particles, both the squark and selectron will decay and end up producing $\tilde{\gamma}$'s.

$$\tilde{e} \to e\tilde{\gamma} \tag{1.3}$$

$$\tilde{q} \to q\tilde{\gamma} \tag{3.12}$$

$$\to q\tilde{g}$$

$$\hookrightarrow q\bar{q}\tilde{\gamma}$$

Furthermore, the measured quantities in deep inelastic ep scattering are the laboratory initial and final electron energies E and E' and the scattering angle θ from which one determines the invariants x, y and Q^2. Then if the decay $\tilde{e} \to e\tilde{\gamma}$ is fast enough, one can still associate E, E' and θ to the final electron, which means integrating over the possible $\tilde{e}$ momenta. We start by writing the cross section for the two step process $1 + 2 \to 3 + 4$ followed by $3 \to a + b$:

$$\sigma = \frac{1}{4\lambda^{1/2}(s, m_1, m_2)} \int d\tilde{p}_3 d\tilde{p}_4\ \frac{ds_3}{2\pi}\ |T_{12\to 34}|^2\ (2\pi)^4 \delta^4(p_1 + p_2 - p_3 - p_4)$$

$$\cdot\, d\tilde{p}_a d\tilde{p}_b \frac{|M_{3\to ab}|^2}{(s_3^2 - m_3^2)^2 + m_3^2\Gamma^2}\ (2\pi)^4 \delta^4(p_3 - p_a - p_b)\ , \tag{3.13}$$

with $\mathcal{M}$, the decay amplitude for $3 \to ab$, $s_3 = p_3^2$ and where

$$\lambda(s, m_1, m_2) = [s - (m_1 + m_2)^2][s - (m_1 - m_2)^2] \ , \tag{3.14}$$

$$d\tilde{p}_i = \frac{d^4 p_i}{(2\pi)^4} \ \delta_+(p_i^2 - m_i^2) \ . \tag{3.15}$$

We use the narrow resonance approximation which consists of replacing the Breit-Wigner resonance by a δ-function and integrating over s_3 immediately:

$$\int \frac{ds_3}{(s_3 - m_3^2)^2 + m_3^2\Gamma^2} \to \frac{1}{2m_3\Gamma} \ .$$

Neglecting final state masses in $\tilde{e} \to e\tilde{\gamma}$, one can write the differential width as $(a = e, \ b = \tilde{\gamma})$

$$d\Gamma = \frac{d^3 p_a}{E_3 E_a} \ \frac{\alpha m_3^2}{2\pi} \ \delta_+(p_b^2) \ , \tag{3.16}$$

which corresponds to a total width for $\tilde{e} \to e\tilde{\gamma}$

$$\Gamma(\tilde{e} \to e\tilde{\gamma}) = \frac{\alpha m_3}{2} \ . \tag{3.17}$$

Finally, using the δ-functions one finds in the electron-quark center of mass

$$d\hat{\sigma} = \frac{|\vec{p}_3|}{(2\pi)^2 \hat{s}\sqrt{\hat{s}}} \int \frac{d^3 p_a}{E_a} \ d\Omega_3^{c.m.} \ |T_{12\to 34}|^2 \ \delta_+((p_3 - p_a)^2) \ , \tag{3.18}$$

where

$$|\vec{p}_3| = \left[\left(\frac{\hat{s} + m_3^2 - m_4^2}{2\sqrt{\hat{s}}} \right)^2 - m_3^2 \right]^{1/2} \ . \tag{3.19}$$

The remaining δ-function in (3.18) corresponds to the requirement that the mass-

less photino be on-shell:

$$(p_3 - p_a)^2 = m_3^2 - 2E_3E_a + 2\vec{p}_3 \cdot \vec{p}_a \tag{3.20}$$

$$E_3 - E_a \geq 0 \ . \tag{3.21}$$

Usually one associates the z-axis with the beam axis by setting

$$p_{1,2} = \frac{\sqrt{s}}{2}(1;\ \pm 1,\ 0,\ 0) \ .$$

In our case, it is more convenient to set the z-axis parallel to $\vec{p}_a$. This amounts to a simple rotation; then

$$p_a = |\vec{p}_a|(1;\ 1,\ 0,\ 0).$$

Accordingly,

$$\begin{aligned} p_{1,2} &= \frac{\sqrt{s}}{2}(1;\ \pm\cos\theta, \pm\sin\theta,\ 0) \ , \\ p_3 &= (E_3, |\vec{p}_3|\cos\theta_3,\ |\vec{p}_3|\sin\theta_3\cos\phi_3,\ |\vec{p}_3|\sin\theta_3\sin\phi_3) \ , \end{aligned} \tag{3.22}$$

with $d\Omega_3^{c.m.} = d\phi_3\ d(\cos\theta_3)$, $d\Omega_4^{c.m.} \to 2\pi d(\cos\theta)$ and

$$(p_3 - p_a)^2 = m_3^2 - 2|\vec{p}_a|(E_3 - |\vec{p}_3|\cos\theta_3) = 0 \ . \tag{3.23}$$

Futhermore, in $ep \to eX$ scattering, one measures Q^2 which corresponds here to

$\hat{t}_{a1} = (p_a - p_1)^2$ not $\hat{t}_{13}$ (see Fig. 3). Since

$$\hat{t}_{a1} = -\sqrt{\hat{s}}|\vec{p}_a|(1 - \cos\theta) \ , \tag{3.24}$$

it is easy to recover the appropriate differential cross section

$$\frac{d\hat{\sigma}^s}{d\hat{t}_{a1}} = \frac{1}{(2\pi\hat{s})^2} \int \frac{d|\vec{p}_a|}{|\vec{p}_a|} \, d\phi_3 \ |T_{12\to 34}|^2 \ . \tag{3.25}$$

We then write $\hat{t}_{13}$ as

$$\hat{t}_{13} = \alpha + \beta\cos\phi_3 \ , \tag{3.26}$$

with

$$\begin{aligned} \alpha &= m_3^2 - \sqrt{\hat{s}}E_3 + \sqrt{\hat{s}}|\vec{p}_3|\cos\theta \ \cos\theta_3 \ , \\ \beta &= \sqrt{\hat{s}}|\vec{p}_3|\sin\theta \ \sin\theta_3 \ , \end{aligned} \tag{3.27}$$

and θ , θ_3 and $|\vec{p}_3|$ given by (3.24), (3.23) and (3.19) to obtain a more convenient form for (3.25):

$$\frac{d\hat{\sigma}^s}{d\hat{t}_{a1}} = \frac{1}{(2\pi\hat{s})^2} \int \frac{d|\vec{p}_a|}{|\vec{p}_a|} \int d\hat{t}_{13} \frac{\beta}{[\beta^2 - (\hat{t}_{13} - \alpha)^2]^{1/2}} |T_{12\to 34}|^2 \ . \tag{3.29}$$

The integration over $\hat{t}_{13}$ can be performed analytically. We present the result in the Appendix. Obviously, $\hat{t}_{13}$ is constrained to values $\alpha - \beta \leq \hat{t}_{13} \leq \alpha + \beta$ in the integration.Moreover, for $A \neq B$, the expression in (3.10) must be positive, thus requiring

$$\max\{\ \alpha - \beta, \eta - \chi\} \ \leq \hat{t}_{13} \leq \ \min\{\ \alpha + \beta, \eta + \chi\} \tag{3.29}$$

with

$$\begin{aligned} \eta &= -\frac{1}{2}(\hat{s} - m_3^2 - m_4^2) \\ \chi &= \frac{1}{2}(\eta^2 - 4m_3^2 \ m_4^2)^{1/2} \ . \end{aligned} \tag{3.30}$$

We integrate over $|\vec{p}_a|$ numerically. The limits of integration are set by relations (3.20 - 3.21) and (3.24)

$$\max\left\{\frac{-\hat{t}_{a1}}{2\sqrt{\hat{s}}},\ \frac{E_3-|\vec{p}_3|}{2}\right\} \leq |\vec{p}_a| \leq \frac{E_3+|\vec{p}_3|}{2}\ . \tag{3.31}$$

Finally, the total cross section associated with subprocesses (2.2) and , (3.9) and (1.3) is obtained by substituting

$$\frac{d\hat{\sigma}_{iA}}{d\hat{t}} \rightarrow \left(\frac{d\hat{\sigma}_{iA}}{d\hat{t}}+\frac{d\hat{\sigma}^s_{iA}}{d\hat{t}}\right) \tag{3.32}$$

in equation (2.6).

4. Results and Discussion

The cross sections are evaluated using the parametrization of $f_i(x,Q^2)$ given by Glück, Hoffman and Reya.[8] The choice of parameterization is not crucial here (as long as it extends to energies expected at SSC) since we only require the quark distributions which are fairly well accounted for in most parametrizations. Moreover, we present here only results for various asymmetries which are less sensitive to the magnitude of the distributions than the cross sections are.

We choose, somewhat arbitrarily, to compute the asymmetries for $x=\frac{1}{3}$ at center of mass energies of HERA (30 GeV $\times$ 820 GeV), i.e. $\sqrt{s}=314$ GeV, and of a 30 GeV $\times$ 20 TeV facility at SSC which corresponds to $\sqrt{s}=1550$ GeV. This last choice is motivated by experimental restrictions on the polarized electron beam energy: Electrons in accelerator rings acquire polarization naturally due to a mechanism related to quantum fluctuations in magnetic fields,[9] but above 40 GeV, little useful polarization remains.

In Figs. 4a-c, we present the results for the asymmetries $A^{\pm}$, $B^{L,R}$ and C for the selectron and squark masses $m_3 = m_4 = 20$ GeV and for gauge fermion masses such as described in Section 3, i.e. $M_{\tilde{\gamma}} = 0$ and $M_{\tilde{Z}} = M_Z$. The notation is the same for all curves in Figs. 4 (and also to Figs. 5 and 6): The standard model predictions are represented by the dotted and dashed lines for HERA and SSC respectively whereas the solid and dot-dashed lines show the calculations including the contribution of (3.9) and (1.3). The supersymmetric effects on A^- are rather small, not larger than 6% for HERA and of the order of 1% at SSC. The polarization asymmetry for positron scattering, A^+, is more interesting. In this case, we clearly see a dip in the asymmetry which corresponds to deviations of up to 11% at HERA and $\simeq 4\%$ at SSC. Both in the limits of $y \to 1$ and $y \to 0$, the supersymmetric effects vanish. This behaviour can be understood on the basis of the phase space available. The small y region corresponds to $\cos\theta \simeq 1$ in which case β in (3.27) also becomes small and the interval of integration over $\hat{t}_{13}$ set by relation (3.29) vanishes. On the other hand, the behaviour as $y \to 1$ is characterized by relation (3.31). According to (3.31), one must have

$$\frac{-\hat{t}_{a1}}{2\sqrt{\hat{s}}} \leq \frac{E_3 + |\vec{p}_3|}{2}$$

which corresponds (for $m_3 = m_4$) to:

$$y \leq \frac{1}{2}\left\{ 1 + \sqrt{1 - \frac{4m_3^2}{\hat{s}}} \right\} \leq 1 \,. \tag{4.1}$$

The same behaviour shows up in $B^{L,R}$ and C (see Figs. 4b-c) since this is essentially a property of the cross sections. In fact, the quantities $B^{L,R}$ and C seem to be more sensitive to the introduction of SUSY interactions. However,

they require that data on both e^-p and e^+p collisions be available in order to be able to make a statement. Finally, another characteristic of the $A^{\pm}$ is that the effects appear to decrease as the energy increases; this is apparently not the case for $B^{L,R}$ and C.

Next we vary two of the input parameters: the masses of the selectron and squark and the mass of the $\tilde{Z}$. First, we increases the mass of the scalar partners. Figs. 5a-c show the results for $m_3 = m_4 = 50$ GeV. The effects of gauge fermion exchange are of the same order of magnitude as in Figs. 4a-c. As expected from relation (4.1), they vanish for $y \leq y_{\max}$ where $y_{\max}$ is smaller than before especially at HERA where $m_3^2/\sqrt{\hat{s}}$ is small.

We repeat the calculations with a different $\tilde{Z}$ mass keeping $m_3 = m_4 = 20$ GeV (see Figs. 6a-c). The effects of changing $M_{\tilde{Z}}$ seems to more important at $y \simeq 0$ and for the HERA case. Such mass effects are understood on the basis of equations (3.9-10) where the $\tilde{Z}$ mass effects are typical of the ratio $M_{\tilde{Z}}^2/\hat{t}_{13}$.

Whether or not the SUSY effects on the asymmetries can be detected at HERA and SSC depends strongly on the assumptions one is willing to make on the expected luminosity at these facilities and on the cross sections which are steep functions of x and y. For $x = \frac{1}{3}$, and assuming an accuracy of a fraction of a picobarn in the determination of the cross section, the SUSY effects on $A^{\pm}$ could be seen at HERA for a limited range of y's but not at SSC. On the other hand, the variations of $B^{L,R}$ and C should be large enough to be detected at both facilities. For smaller x's, prospects are even more encouraging because of higher statistics.

We conclude by making the following comments. With HERA being built with a polarized electron beam, the process $e^{\pm}_{R,L}p \to e^{\pm}X$ will certainly be the

most thoroughly investigated and should give us a much better idea of the extent to which the standard model can be trusted. Other modifications to the weak interaction theory than that studied in this work (e.g. a second Z_0, composite structure at higher scale, SQCD...) are also bound to show up in the asymmetries. Finally, we are aware that the ep machine at HERA is not the first or even the best available experiment to test the presence of gauge fermions or SUSY in general. In terms of the center-of-mass energy required to produce SUSY particles, both e^+e^- and $\bar{p}p$ machines should reach HERA's capabilities before it comes in operation and, it is believed by most high energy physicists that the best signal for SUSY could come from missing p_T analysis. But missing p_T's are certainly not exclusive to supersymmetric processes and one must also look for other manifestations of SUSY. Furthermore, polarized- $e^{\pm}p$ scattering is certainly one of the best way to test the weak properties of new particles. It is for these reasons that we believe this work is important.

Acknowledgements

The author would like to thank Professor S. D. Drell and the other members of the Theory Group for their hospitality at SLAC. Many thanks also go to E. Massó for useful suggestions in preparing the manuscript. This work was supported by the U.S. Department of Energy and the National Sciences and Engineering Research Council of Canada.

Appendix

The integration over $\hat{t}$ in (3.22) takes the form

$$I = \int \frac{d\tau}{[(\beta^2 - \alpha^2) + 2\alpha\tau - \tau^2]^{1/2}} \; P_2\left(\frac{1}{\tau - \gamma}\right) \tag{A.1}$$

where $P_2(u)$ is at most a polynomial of degree 2 in u. (A1) is easiest to perform with the change of variables

$$u = \frac{1}{\tau - \gamma} \; . \tag{A.2}$$

Then one gets integrals of the type

$$R_n = \int du \; \frac{u^n}{\sqrt{r(u)}} \tag{A3}$$

where $n = 0,\ 1,\ \ldots$ and $r(u) = A + Bu + Cu^2$ with $A,\ B$ and C given by

$$A = -1, \quad B = 2(\alpha - \gamma) \qquad \text{and} \qquad C = \beta^2 - (\alpha - \gamma)^2 \tag{A4}$$

Integrating by parts

$$\begin{aligned} R_1 &= \frac{\sqrt{r(u)}}{C} - \frac{B}{2C} \; R_0 \\ R_2 &= \left(\frac{u}{2C} - \frac{3B}{AC^2}\right) \; \sqrt{r(u)} + \left(\frac{3B^2}{8C^2} - \frac{A}{2C}\right) \; R_0 \; , \ldots \end{aligned} \tag{A5}$$

and

$$R_0 = \frac{1}{\sqrt{-C}} \; \ln \left| 2\sqrt{C r(u)} + 2Cu + B \right| \tag{A6}$$

where $C > 0$. Finally, the coefficient of P_2 in (A.1) are given by rewriting $|T^{AA}|^2$

and $|T^{AB}|^2$ as

$$|T^{AA}|^2 = 4e^4\hat{s}\left[\left(\frac{a^2M_{\tilde{\gamma}}^2}{(\hat{t}_{13}-M_{\tilde{\gamma}}^2)^2}+\frac{2ab_{AA}M_{\tilde{\gamma}}M_{\tilde{Z}}}{(M_{\tilde{\gamma}}^2-M_{\tilde{Z}}^2)(\hat{t}_{13}-M_{\tilde{\gamma}}^2)}\right)+(M_{\tilde{Z}}\leftrightarrow M_{\tilde{\gamma}},\ a\leftrightarrow b_{AA})\right]$$

$$|T^{AB}|^2 = 4e^4\Bigg\{\ (a+b_{AB})^2+\left(a^2\omega(M_{\tilde{\gamma}},M_{\tilde{\gamma}})+\frac{2ab_{AB}\sigma(M_{\tilde{\gamma}},M_{\tilde{Z}})}{(\hat{t}_{13}-M_{\tilde{\gamma}}^2)}+\frac{a^2\sigma(M_{\tilde{\gamma}},M_{\tilde{\gamma}})}{(\hat{t}-13-M_{\tilde{\gamma}}^2)^2}\right)$$

$$(M_{\tilde{Z}}\leftrightarrow M_{\tilde{\gamma}},\ a\leftrightarrow b_{AB})\Bigg\} \qquad (A7)$$

with

$$\omega(M_i,M_j) = M_3^2+M_4^2-\hat{s}-M_i^2-M_j^2$$

$$\sigma(M_i,M_j) = M_i^2M_j^2+M_3^2M_4^2+M_i^2\omega(M_i,M_j)\ .$$

REFERENCES

1. J. Wess and B. Zumino, Nucl. Phys. B70, 39 (1974); P. Fayet and S. Ferrara, Phys. Rep. 32C, 249 (1977).
2. P. Fayet and J. Iliopoulos, Phys. Lett. 51B, 461 (1974); E. Witten, Nucl. Phys. B188, 513 (1981); S. Dimopoulos and H. Georgi, Nucl. Phys. B93, 150 (1981).
3. C. Y. Prescott *et al.*, Phys. Lett. 77B, 347 (1978); 84B, 524 (1979)
4. S. K. Jones and C. H. Llewellyn Smith, Nucl. Phys. B217, 145 (1983); P. Salati and J. C. Walet, Phys. Lett. B122, 397 (1983).
5. J. A. Bagger and M. E. Peskin, Phys. Rev. D 31, 2211 (1985)
6. R. Rückl, Nucl. Phys. B234, 91 (1984).
7. H. E. Haber and G. L. Kane, Phys. Rep. 117, 75 (1985).
8. M. Glück, E. Hoffman and E. Reya, Z. Phys. C13, 119 (1982).
9. A. Sokelov and I. Ternov, Sov. Phys. Dokl. 8, 1203 (1964)

FIGURE CAPTIONS

1. Diagrams contributing to $e^{\pm}p \to e^{\pm}X$ scattering: (a) diagrams for $e^{\pm}q \to e^{\pm}q$ and (b) diagrams for $e^{\pm}q \to \tilde{e}^{\pm}\tilde{q}$.
2. Feynman rules for $q\tilde{q}\tilde{\gamma}$ and $q\tilde{q}\tilde{Z}$ vertices. f stands for any quark or lepton and $\tilde{V}$ for gauge fermions $\tilde{\gamma}$ and $\tilde{Z}$.
3. Kinematics of the reaction $ep \to eX$ via the production of the selectron in $eq \to \tilde{e}\tilde{q}$ followed by the decay $\tilde{e} \to e\tilde{\gamma}$.
4. (a) Polarization asymmetries $A^{\pm}(x,y)$ and (b) $B^{L,R}(x,y)$ and, charge asymmetry $C(x,y)$ in $e^{-}_{L,R}p \to e^{-}X$ as a function of y for $x = 1/3$, $m_3 = m_4 =$ 20 GeV and $M_{\tilde{Z}} = M_Z$. The dotted and dashed curves denote the prediction of the standard model for the ep machines at HERA ($\sqrt{s} = 314$ GeV) and SSC ($\sqrt{s} = 1550$ GeV) respectively ; the solid and dot-dashed curves are for the predictions including SUSY interactions.
5. Same as in Figs. 4 with $m_3 = m_4 = 50$ GeV.
6. Same as in Figs. 4 with $M_{\tilde{Z}} = 60$ GeV.

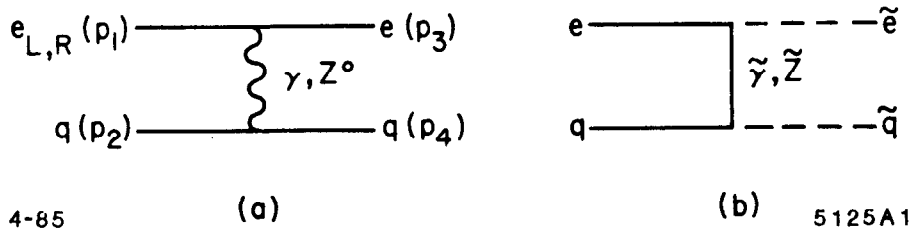

Fig. 1

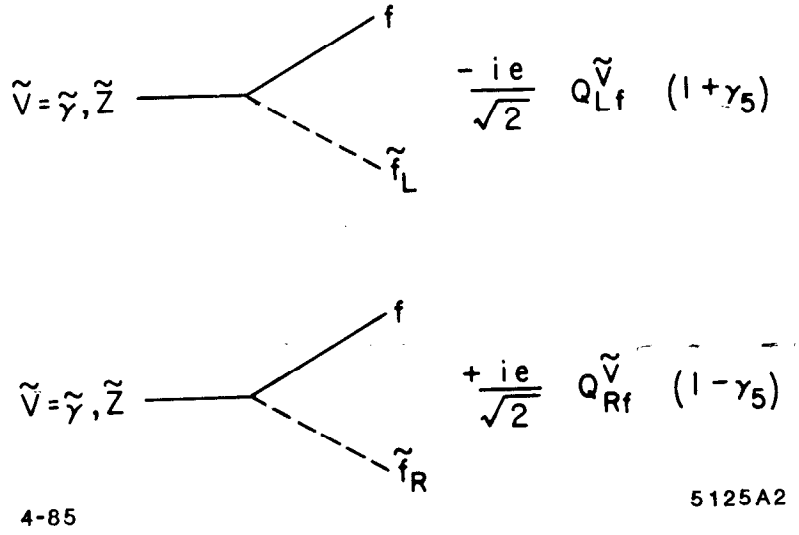
$\tilde{V}=\tilde{\gamma},\tilde{Z}$
f
$\tilde{f}_L$
$\frac{-ie}{\sqrt{2}}\ Q^{\tilde{V}}_{Lf}\ (1+\gamma_5)$
$\tilde{V}=\tilde{\gamma},\tilde{Z}$
f
$\tilde{f}_R$
$\frac{+ie}{\sqrt{2}}\ Q^{\tilde{V}}_{Rf}\ (1-\gamma_5)$
4-85
5125A2

Fig. 2

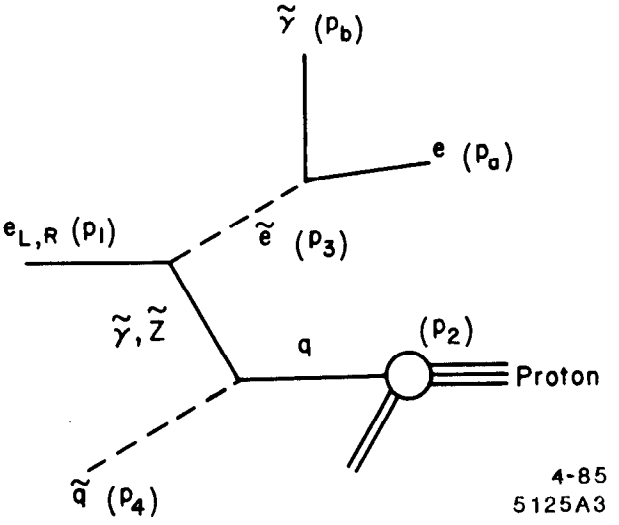
$\tilde{\gamma}$ (p_b)
e (p_a)
$e_{L,R}$ (p_1)
$\tilde{e}$ (p_3)
$\tilde{\gamma},\tilde{Z}$
q
(p_2)
Proton
$\tilde{q}$ (p_4)
4-85
5125A3

Fig. 3

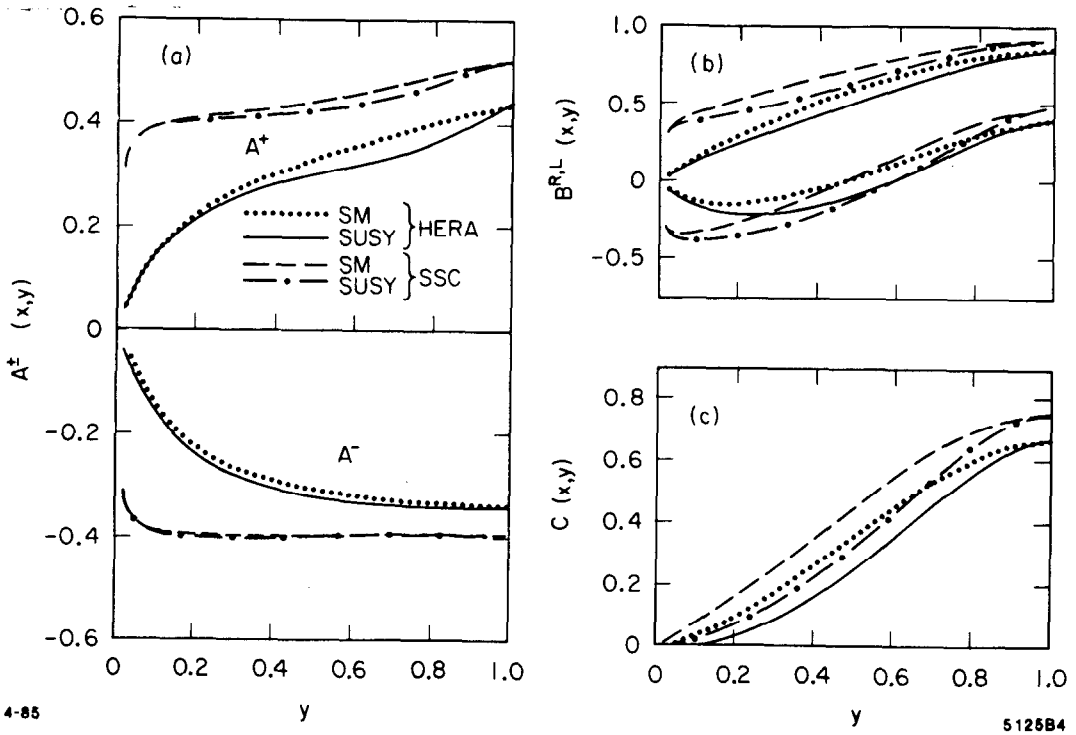
(a)
A+
A-
SM
SUSY
HERA
SM
SUSY
SSC
A± (x,y)
0.6
0.4
0.2
0
-0.2
-0.4
-0.6
0
0.2
0.4
0.6
0.8
1.0
y
4-85
(b)
B^R,L (x,y)
1.0
0.5
0
-0.5
(c)
C (x,y)
0.8
0.6
0.4
0.2
0
0
0.2
0.4
0.6
0.8
1.0
y
5125B4

Fig. 4

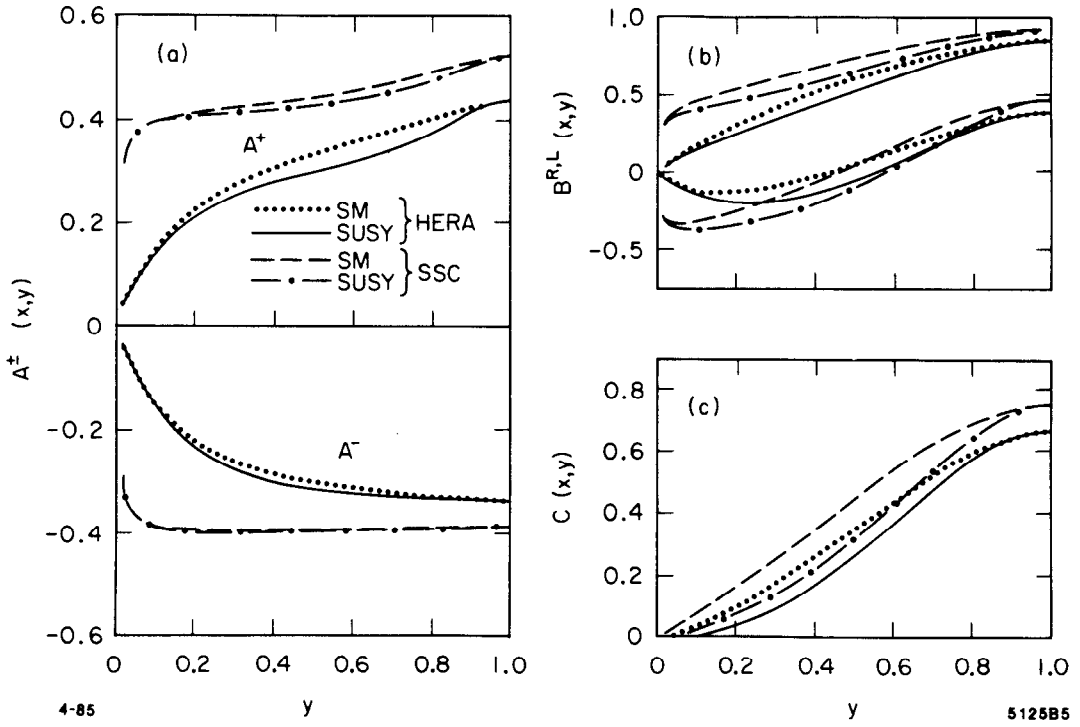
(a)
A+
A−
SM
SUSY
HERA
SM
SUSY
SSC
A± (x,y)
0.6
0.4
0.2
0
-0.2
-0.4
-0.6
0
0.2
0.4
0.6
0.8
1.0
y
4-85
(b)
B^R,L (x,y)
1.0
0.5
0
-0.5
(c)
C (x,y)
0.8
0.6
0.4
0.2
0
y
5125B5

Fig. 5

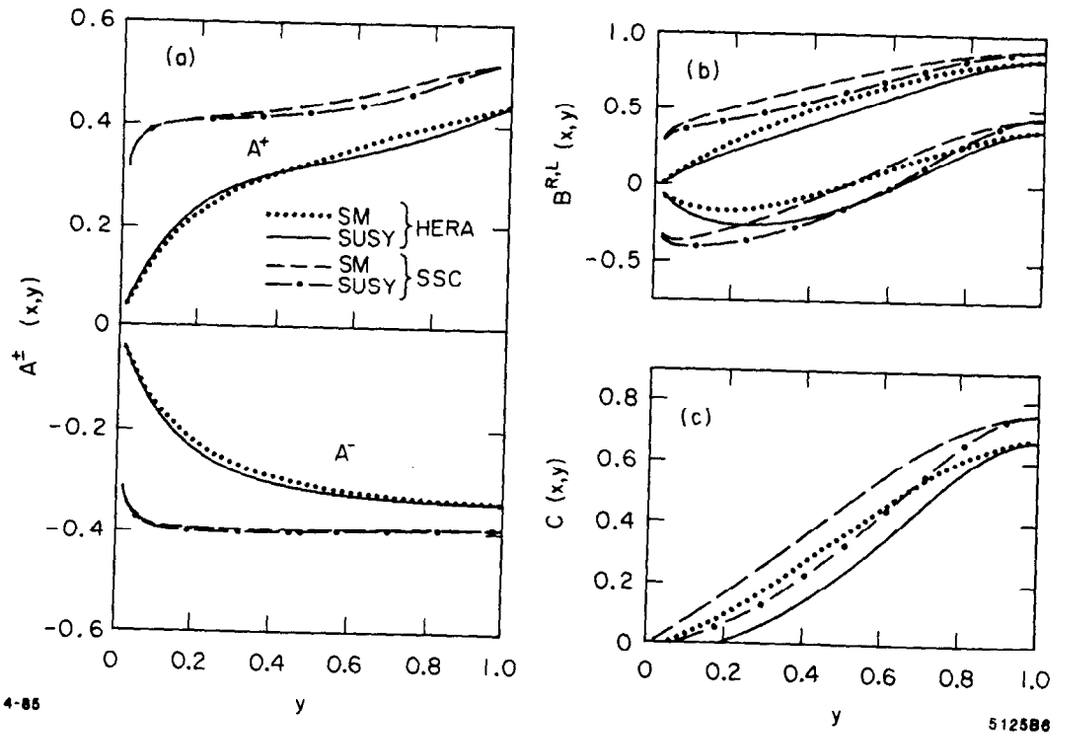

Fig. 6